Routes of phosphoryl group transfer during signal transmission and signal decay in the dimeric sensor histidine kinase ArcB

Received for publication, May 9, 2018, and in revised form, June 14, 2018 Published, Papers in Press, June 26, 2018, DOI 10.1074/jbc.RA118.003910

Juan L. Teran-Melo[‡], Gabriela R. Peña-Sandoval[§], Hortencia Silva-Jimenez[¶], Claudia Rodriguez[‡], Adrián F. Alvarez[‡], and Dimitris Georgellis[‡1]

From the [‡]Departamento de Genética Molecular, Instituto de Fisiología Celular Universidad Nacional Autónoma de México, 04510 Mexico City, Mexico, the [§]Unidad Académica de Agricultura, Universidad Autónoma de Nayarit, 63190 Tepic, Nayarit, Mexico, and the [¶]Area de Oceanografía Química, Instituto de Investigaciones Oceanológicas, Universidad Autónoma de Baja California, 22860 Ensenada, Baja California, Mexico

Edited by Chris Whitfield

The Arc (anoxic redox control) two-component system of *Escherichia coli*, comprising ArcA as the response regulator and ArcB as the sensor histidine kinase, modulates the expression of numerous genes in response to respiratory growth conditions. Under reducing growth conditions, ArcB autophosphorylates at the expense of ATP, and transphosphorylates ArcA via a $His^{292} \rightarrow Asp^{576} \rightarrow His^{717} \rightarrow Asp^{54}$ phosphorelay, whereas under oxidizing growth conditions, ArcB catalyzes the dephosphorylation of ArcA-P by a reverse $Asp^{54} \rightarrow His^{717} \rightarrow Asp^{576} \rightarrow P_i$ phosphorelay. However, the exact phosphoryl group transfer routes and the molecular mechanisms determining their directions are unclear. Here, we show that, during signal propagation, the $His^{292} \rightarrow Asp^{576}$ and $Asp^{576} \rightarrow His^{717}$ phosphoryl group transfers within ArcB dimers occur intra- and intermolecularly, respectively. Moreover, we report that, during signal decay, the phosphoryl group transfer from His^{717} to Asp^{576} takes place intramolecularly. In conclusion, we present a mechanism that dictates the direction of the phosphoryl group transfer within ArcB dimers and that enables the discrimination of the kinase and phosphatase activities of ArcB.

The Arc two-component signal transduction system plays an important role in the transcriptional regulatory network that allows facultative anaerobic bacteria, such as *Escherichia coli*, to sense and signal changes in respiratory growth conditions and to adapt their gene expression accordingly (1–4). This system consists of the cytoplasmic response regulator ArcA, and the membrane-anchored sensor kinase ArcB (5, 6). ArcA is a typical response regulator, possessing an N-terminal receiver domain with a phosphoryl group–accepting Asp residue at position 54 and a C-terminal helix-turn-helix DNA-binding domain. In contrast, ArcB is an unorthodox sensor kinase that contains three catalytic cytosolic domains: a transmitter domain (H1) with a conserved His^{292} residue, a central receiver domain (D1) with a conserved Asp^{576} residue, and a C-terminal histidine phosphotransfer domain (H2) with a conserved His^{717} residue (6, 7). In addition, the ArcB protein contains a functional leucine zipper (8) and a PAS domain (9), both located in the linker region, which is the segment connecting the transmembrane domain with the transmitter domain.

Under reducing growth conditions, ArcB autophosphorylates in an ATP-dependent manner, a process that is enhanced by certain anaerobic metabolites, such as D-lactate, acetate, and pyruvate (10, 11), and transphosphorylates ArcA via a $His^{292} \rightarrow Asp^{576} \rightarrow His^{717} \rightarrow Asp^{54}$ phosphorelay (12, 13). Phosphorylated ArcA (ArcA-P),[2] in turn, represses the expression of many operons involved in respiratory metabolism and activates some others encoding proteins involved in fermentative metabolism (14–17). Under oxic growth conditions, ArcB acts as a specific ArcA-P phosphatase, catalyzing the dephosphorylation of ArcA-P by a reverse $Asp^{54} \rightarrow His^{717} \rightarrow Asp^{576} \rightarrow P_i$ phosphorelay (18, 19). The catalytic activity of ArcB has been shown to be set by rotational movements that alter the orientation of the cytosolic portion of ArcB (20). Moreover, the molecular event for ArcB regulation involves the oxidation or reduction of two cytosol-located redox-active cysteine residues that participate in intermolecular disulfide bond formation, a reaction in which the quinol/quinone electron carriers act as the direct oxidants or reductants (21–24).

In general, histidine sensor kinases act as homodimers (25–28) and autophosphorylate by either an inter- or intramolecular reaction (29–35). Also, studies on the subsequent phosphoryl group (~P) transfer steps (*i.e.* from H1 to D1 and from D1 to H2) in various hybrid histidine kinases indicate that they can occur either intra- or intermolecularly, depending on the particular sensor kinase protein and on the specific ~P transfer step (36–38). In contrast, the ~P transfer step from H2 to D1 in

This work was supported by a doctoral fellowship from the Consejo Nacional de Ciencia y Tecnología (CONACyT) (to J. L. T. M.) as well as DGAPA-PAPIIT, UNAM, Grants IN208718 and IN209918 (to A. F. A. and D. G.). The authors declare that they have no conflicts of interest with the contents of this article.

This article contains Table S1 and Figs. S1–S3.

[1] To whom correspondence should be addressed: Instituto de Fisiología Celular, Universidad Nacional Autónoma de México, 04510 Mexico City, Mexico. Tel.: 52-55-5622-5738; Fax: 52-55-5622-5611; E-mail: dimitris@ifc.unam.mx.

[2] The abbreviations used are: ArcA-P, phosphorylated ArcA; ~P, phosphoryl group; MBP, maltose-binding protein; β-gal, β-galactosidase; IPTG, isopropyl 1-thio-β-D-galactopyranoside; LB, lysogeny broth; NTA, nitrilotriacetic acid.

the reverse phosphorelay, responsible for the phosphatase activity of these hybrid sensor kinases, has yet to be addressed.

In the case of ArcB, the autophosphorylation reaction appears to occur intramolecularly, as the γ-phosphoryl group of ATP bound to one monomer in the homodimer was shown to be transferred to the histidine of the same monomer (35, 38). In contrast, the mode of ~P transfer in the two subsequent steps in ArcB signaling remains ambiguous, because two independent studies reached dissimilar conclusions (38, 39). On one hand, in a report based on *in vivo* experiments analyzed with mathematical and statistical models, it was suggested that a bimolecular or allosteric mechanism, in which the integrity of all phospho-accepting/donating sites is required and in which no exclusive intra- or intermolecular ~P transfer mechanisms are identifiable, may be operating during ArcB signaling (39). On the other hand, in a later study based on *in vitro* complementation analyses, it was proposed that the ~P transfers from H1 to D1 and from D1 to H2 occur intermolecularly (38).

Here, we present results from *in vitro* and *in vivo* experiments addressing the above mentioned discrepancy and extend these studies to include the characterization of the H2 to D1 ~P transfer step, involved in ArcA-P dephosphorylation during signal decay. Our results demonstrate that the ~P transfer from H1 to D1 occurs exclusively intramolecularly, whereas the following step (*i.e.* from D1 to H2) occurs preferentially intermolecularly. Finally, the H2 to D1 ~P transfer, responsible for signal decay, shows a clear preference for the intramolecular reaction. The consequences of the proposed ~P transfers between the various ArcB modules for the regulation of signal transmission and signal decay of the Arc two-component system are discussed.

Results

Probing the mode of phosphoryl group transfer from the transmitter domain to the receiver domain of ArcB

Autophosphorylation of the tripartite sensor kinase ArcB was shown to be an intramolecular reaction (35, 38), whereas contradictory results were reported for the mode of ~P transfer in the two subsequent steps (38, 39). Therefore, we attempted to probe the mode of these ~P transfer steps by an approach different from the ones used previously.

To this end, we generated N-terminal His_6-tagged cytosolic WT and mutant ArcB variants (hereafter referred to as His_6-H1-D1-H2), carrying single or multiple punctual mutations of the conserved phosphorylation sites. In other words, the conserved histidine 292 in H1 was replaced by glutamine (hereafter referred to as H1*), the conserved aspartate 576 in D1 was replaced by alanine (hereafter referred to as D1*), and the conserved histidine 717 in H2 was replaced by glutamine (hereafter referred to as H2*). WT and single- and multiple-mutant His_6-H1-D1-H2 proteins were purified, and their ability to autophosphorylate and transphosphorylate His_6-ArcA (hereafter referred to as ArcA) was tested. ArcA was rapidly phosphorylated by His_6-H1-D1-H2 (Fig. 1*A*), but not by His_6-H1*-D1-H2, His_6-H1-D1*-H2, His_6-H1-D1-H2*, or His_6-H1*-D1*-H2 mutant proteins (Fig. S1, *A–D*), in agreement with previous reports (12, 13). The ability of combinations of mutant His_6-H1-D1-H2 variants to transphosphorylate ArcA was then evaluated. No ArcA phosphorylation was observed in the reaction mixture containing His_6-H1*-D1-H2 and His_6-H1-D1*-H2, in which only intermolecular H1 to D1 phosphotransfer is allowed (Fig. 1, *B* and *D*). On the other hand, a weak ArcA phosphorylation, ~30% of that observed by the WT His_6-H1-D1-H2, was obtained in the reaction mixture containing His_6-H1*-D1*-H2 and His_6-H1-D1-H2*, in which only the intramolecular H1 to D1 ~P transfer is permitted (Fig. 1, *C* and *D*), indicating that the ~P transfer from H1 to D1 occurs intramolecularly. However, this conclusion is hampered by the fact that none of the combinations was able to restore the phosphorelay at WT ArcB levels, most likely due to the insufficient heterodimer formation in the reaction mixture.

To ensure heterodimer formation, a set of plasmids carrying arabinose-inducible MBP-tagged H1-D1-H2 variants were constructed and transformed in strains harboring plasmids that

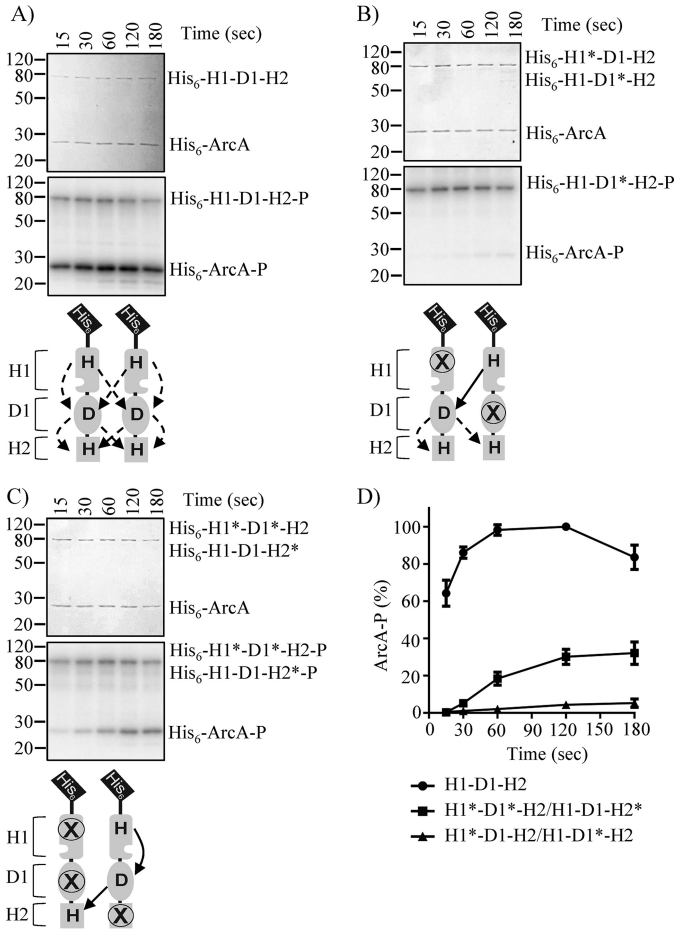

Figure 1. ArcA phosphorylation by His_6-ArcB$^{78-778}$ and by combinations of His_6-ArcB$^{78-778}$ phosphorelay mutants. Purified ArcA was incubated in a 30-μl reaction mixture with [γ-^{32}P]ATP and His_6-H1-D1-H2 (*A*), His_6-H1*D1-H2 and His_6-H1-D1*-H2 (*B*), or His_6-H1*-D1*-H2 and His_6-H1-D1-H2* (*C*). At the indicated time intervals, 5-μl samples were withdrawn and subjected to SDS-PAGE analysis. Coomassie Blue-stained gels revealing protein bands (*top panels*), corresponding autoradiograms (*middle panels*), and schemes showing the permitted ~P transfers into ArcB dimers (*bottom panels*) are presented. The molecular mass standard values (kDa) are shown on the *left*, and the position of each polypeptide in the gel is indicated on the *right* of each *panel*. *D*, relative amount of ArcA-P formed, as quantified by densitometric analysis of the autoradiogams. Data represent the averages from at least three independent experiments, and S.D. values (*error bars*) are indicated.

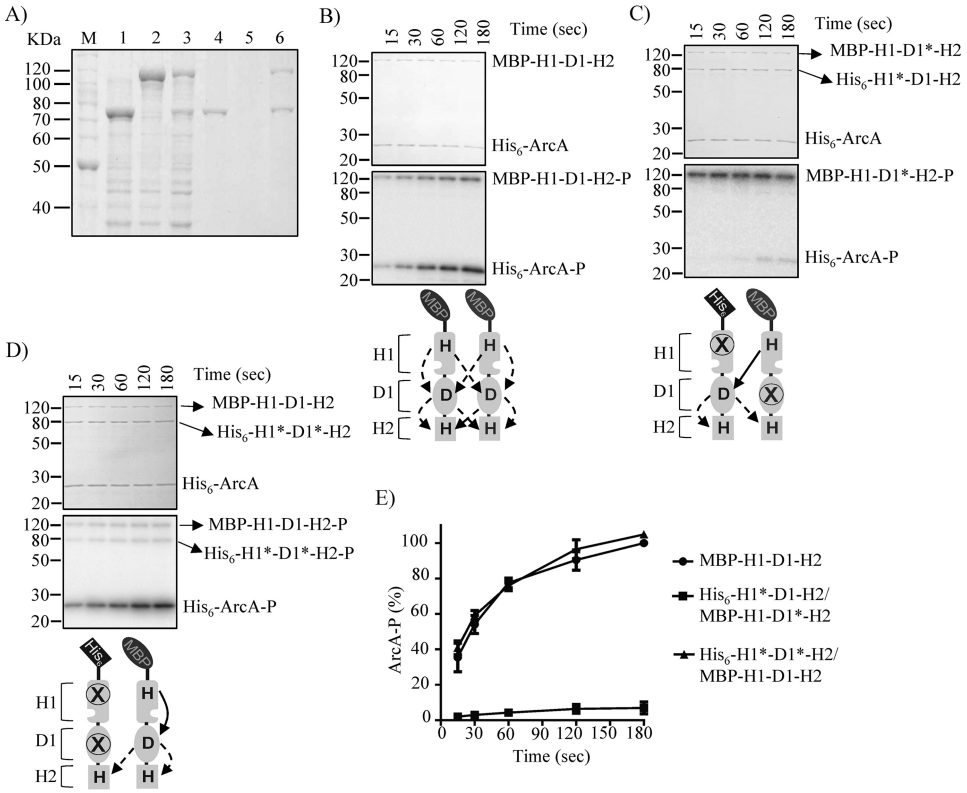

Figure 2. Probing the mode of H1 to D1 ~P group transfer by *in vitro* phosphorelay complementation assays using His_6-$ArcB^{78-778*}$/MBP-$ArcB^{78-778*}$ dimers. *A*, overexpression of His_6-H1*-D1-H2 (*lane 1*), MBP-H1-D1*-H2 (*lane 2*), and His_6-H1*-D1-H2/MBP-H1-D1*-H2 (*lane 3*) was analyzed by SDS-PAGE and Coomassie Blue staining. Overexpressed proteins were purified by Ni-NTA affinity chromatography, and the elution fractions of His_6-H1*-D1-H2 (*lane 4*), MBP-H1-D1*-H2 (*lane 5*), and His_6-H1*-D1-H2/MBP-H1- D1*-H2 (*lane 6*) were analyzed by SDS-PAGE and visualized by Coomassie Blue staining. Purified ArcA was incubated in a 30-μl reaction mixture with [γ-^{32}P]ATP and purified/co-eluted MBP-H1-D1-H2 (*B*), His_6-H1*-D1-H2/MBP-H1-D1*-H2 (*C*), or His_6-H1*-D1*-H2/MBP-H1-D1-H2 (*D*). At the indicated time intervals, 5-μl samples were withdrawn and subjected to SDS-PAGE analysis. Coomassie Blue-stained gels revealing protein bands (*top panels*), the corresponding autoradiograms (*middle panels*), and schemes showing the permitted ~P transfers (*bottom panels*) are presented. The molecular mass standard values (kDa) are shown on the *left*, and the position of each polypeptide in the gel is indicated on the *right* of each *panel*. *E*, relative amount of ArcA-P formed, as quantified by densitometric analysis of the autoradiograms. Data represent the averages from at least three independent experiments, and the S.D. values (*error bars*) are indicated.

express complementary His_6-tagged H1-D1-H2 mutant proteins. The desired combinations of MBP-tagged and His_6-tagged protein versions were simultaneously overexpressed and purified under native conditions, using Ni-NTA affinity chromatography. According to this approach, only His_6-tagged/MBP-tagged protein heterodimers and His_6-tagged protein homodimers should be purified, and MBP-tagged protein homodimers should not be. An example of this approach is presented in Fig. 2*A*. The obtained results demonstrate that His_6-H1*-D1-H2 and MBP-H1-D1*-H2 were readily overexpressed (Fig. 2*A*, *lanes 2* and *3*) and that only His_6-H1*-D1-H2, and not MBP-H1-D1*-H2, was retained by and eluted from the nickel-nitrilotriacetic acid resin (Fig. 2*A*, *lanes 5* and *6*). However, when both proteins were co-expressed (Fig. 2*A*, *lane 4*), the MBP-H1-D1*-H2 protein co-eluted with His_6-H1*-D1-H2 to almost stoichiometric amounts (Fig. 2*A*, *lane 7*), ensuring heterodimer formation.

Single MBP-tagged proteins, used for heterodimer formation, were purified and subjected to *in vitro* phosphorylation assays with [γ-^{32}P]ATP and His_6-ArcA. Only the MBP-tagged proteins having a WT H1 were able to autophosphorylate (Fig. S1*E*), and only the MBP-H1-D1-H2 was able to transphosphorylate ArcA (Fig. 2*B*), indicating that the purified proteins have the expected activities and that the N-terminal MBP tag does not interfere with the activity of ArcB. Subsequently, the ability of the His_6-H1*-D1-H2/MBP-H1-D1*-H2 heterodimer, in which only intermolecular phosphoryl group transfer from H1 to D1 is permitted, to functionally complement and restore the phosphorelay to ArcA was tested (Fig. 2*C*). Although the MBP-H1-D1*-H2 protein was rapidly autophosphorylated, no His_6-H1*-D1-H2-P was observed, and almost no ArcA-P was formed (Fig. 2, *C* and *E*), suggesting that the H1 to D1 phosphotransfer does not occur intermolecularly. In contrast, the His_6-H1*-D1*-H2/MBP-H1-D1-H2 heterodimer was found to readily transphosphorylate ArcA (Fig. 2, *D* and *E*), indicating that the phosphoryl group transfer from H1 to D1 occurs intramolecularly, at least *in vitro*. It has to be noted that phosphorylation of His_6-H1*-D1*-H2 was also observed, most likely due to intermolecular phosphoryl group transfer from D1 to H2 or from ArcA to H2.

To verify the *in vitro* results by *in vivo* experiments, low-copy number plasmids carrying the $arcB^{H292Q,D576A}$ (pEXT22 $CmArcB^{H292Q,D576A}$) and $arcB^{H292Q}$ (pEXT22$CmArcB^{H292Q}$) mutant alleles were generated and transformed, respectively, into the $arcB^{H717Q}$ (IFC2002) and $arcB^{D576A}$ (IFC2001) mutant strains, both carrying a $\lambda\Phi$(*cydA′-lacZ*) reporter (40). Plasmid pEXT22, which was reported to have 1–2 copies/cell (41), and *arcB* mutant alleles under the control of the native *arcB* pro-

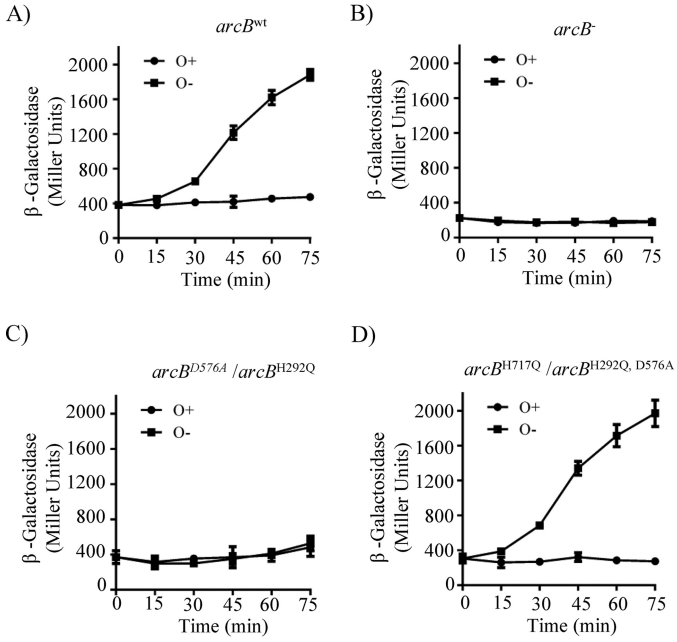

Figure 3. Co-expression of *arcB*H717Q and *arcB*H292Q,D576A restores ArcB activity and regulation of reporter expression. Cultures of strain ECL5003 (*arcB*^{wt}) (*A*) and its isogenic strains ECL5004 (*arcB*$^{-}$) (*B*) and IFC2001 (*arcB*^{D576A}) (*C*) harboring plasmid pEXT22CmArcB^{H292Q} and IFC2002 (*arcB*^{H717Q}) (*D*) harboring plasmid pEXT22CmArcB^{H292Q,D576A}, all carrying the ArcA-P–activatable λΦ(*cydA′-lacZ*) reporter, were grown aerobically in LB buffered with 0.1 M MOPS (pH 7.4) and supplemented with 20 mM D-xylose. At an A_{600} of 0.2, one aliquot was withdrawn, to measure the β-gal activity (depicted as 0 min), and the rest of the culture was divided in two. One part was kept under aerobic conditions (*circles*) as a control, whereas the other was shifted to anaerobiosis (*squares*), and the time course of the β-gal activity was followed. The data represent the averages from three independent experiments, and the S.D. values (*error bars*) are indicated.

moter were chosen to avoid the overexpression of the sensor kinase. This is because distortion of the ArcB/ArcA concentration balance has been reported to produce unpredictable effects on reporter expression (42). Indeed, Western blot analysis using ArcB polyclonal antibodies, raised against purified His$_6$-ArcB$^{78-520}$ (40), revealed that all plasmid-borne *arcB* alleles produce similar to WT levels of ArcB protein (Fig. S2*E*). Subsequently, the phenotypic consequences of the above described strains were analyzed by changes in the *in vivo* levels of phosphorylated ArcA, as indicated by the expression of the ArcA-P–activatable λΦ(*cydA′-lacZ*) reporter (Fig. 3). As expected, *arcB*-null phenotypes were found for strains IFC2002 (*arcB*^{H717Q}) and IFC2001 (*arcB*^{D576A}) and when the plasmid-borne *arcB*^{H717Q,D576A} and *arcB*^{H292A} were expressed in the Δ*arcB* mutant strain ECL5004 (Fig. S2, *A–D*), in agreement with the *in vitro* results and previous reports (12). Moreover, expression of the plasmid-borne *arcB*^{H292Q} in IFC2001 (*arcB*^{D576A}), where only intermolecular ~P transfer from H1 to D1 is permitted, resulted in an *arcB*-null phenotype (Fig. 3, *B* and *C*). In contrast, expression of the plasmid-borne *arcB*^{H292Q,D576A} in IFC2002 (*arcB*^{H717Q}), where only intramolecular phosphoryl group transfer from H1 to D1 is permitted, resulted in WT levels of reporter expression (Fig. 3, *A* and *D*), in accordance with the above presented *in vitro* results. Therefore, it appears reasonable to conclude that an intramolecular mode of ~P transfer operates from H1 to D1. This result also suggests that the *in vivo* ~P transfer from D1 to H2 occurs intermolecularly, although the intramolecular mode cannot be excluded. Taken together, the above results from the *in vitro* and *in vivo* experiments provide strong evidence that the phosphorelay along ArcB comprises an intramolecular H1 to D1 ~P transfer.

Probing the mode of ~P transfer from D1 to H2 within the ArcB dimer

We then asked whether the D1 to H2 ~P transfer step within ArcB dimers occurs intra- or intermolecularly. To this end, the His$_6$-H1-D1-H2*/MBP-H1*-D1*-H2 heterodimer, permitting intermolecular ~P transfer, and His$_6$-H1*-D1*-H2*/MBP-H1-D1-H2 heterodimer, permitting intramolecular ~P transfer, were obtained, and their ability to complete the phosphorelay and transphosphorylate ArcA was evaluated. His$_6$-H1-D1-H2*/MBP-H1*-D1*-H2 was found to phosphorylate ArcA at WT ArcB levels, whereas the His$_6$-H1*-D1*-H2*/MBP-H1-D1-H2 heterodimer phosphorylated ArcA at a significantly lower rate (Fig. 4). In contrast, homodimers composed by any of the ArcB mutant variants were unable to phosphorylate ArcA (Fig. S1). These results indicate that the D1 to H2 ~P transfer step occurs preferentially intermolecularly *in vitro*, in agreement with a previous study (38). Indeed, in the above presented *in vivo* complementation assay, co-expression of the *arcB*^{H717Q} and *arcB*^{H292Q,D576A} mutant alleles resulted in WT levels of reporter expression (Fig. 3*D*), indicating that an intermolecular D1 to H2 phosphotransfer does occur during *in vivo* ArcB signaling. The direct evaluation of an intramolecular ~P transfer from D1 to H2 *in vivo*, requiring the expression of ArcB^{D576A,H717Q} and ArcB^{H292A}, however, is unattainable because the ~P transfer step from H1 to D1 is exclusively intramolecular, rendering the use of a WT ArcB mandatory, which, in turn, impedes the discrimination between the two modes of ~P transfer. To circumvent this problem, we reasoned that expression of increasing amounts of *arcB*^{D576A,H717Q} in an *arcB*^{wt} background strain should favor ArcB^{D576A,H717Q}/ArcB^{wt} heterodimer formation. Because such heterodimers allow only intramolecular D1 to H2 phosphotransfer, a reduction of the ArcA-P levels should be obtained if an intermolecular D1 to H2 ~P transfer were to be favored. Because overexpression of a sensor kinase may have unexpected effects on its signaling, increased concentrations of *arcB*^{H292Q,D576A} in the *arcB*^{wt} background, favoring the formation of ArcB^{H292Q,D576A}/ArcB^{wt} heterodimers that permit both inter- and intramolecular D1 to H2 phosphotransfer, was used as a control.

To this end, plasmids pBADArcB^{H292Q,D576A} and pBAD ArcB^{D576D,H717A}, carrying, respectively, the *arcB*^{H292Q,D576A} and *arcB*^{D576A,H717Q} mutant alleles under the control of the inducible arabinose promoter were constructed and transformed into the ECL5003 strain, which carries the ArcA-P–activatable λΦ(*cydA′-lacZ*) reporter (12). The transformants were grown anaerobically in the presence of various concentrations of arabinose (0–30 μM), and at midexponential phase of growth, A_{600} of ~0.5, the β-gal activities were determined (Fig. 5). Increasing amounts of inductor in the growth medium of the strain carrying the ArcB^{H292Q,D576A}-expressing plasmid resulted in decreasing levels of reporter expression (Fig. 5). Because the intramolecular H1 to D1 phosphotransfer and both modes of phosphotransfer from D1 to H2 are permitted within the

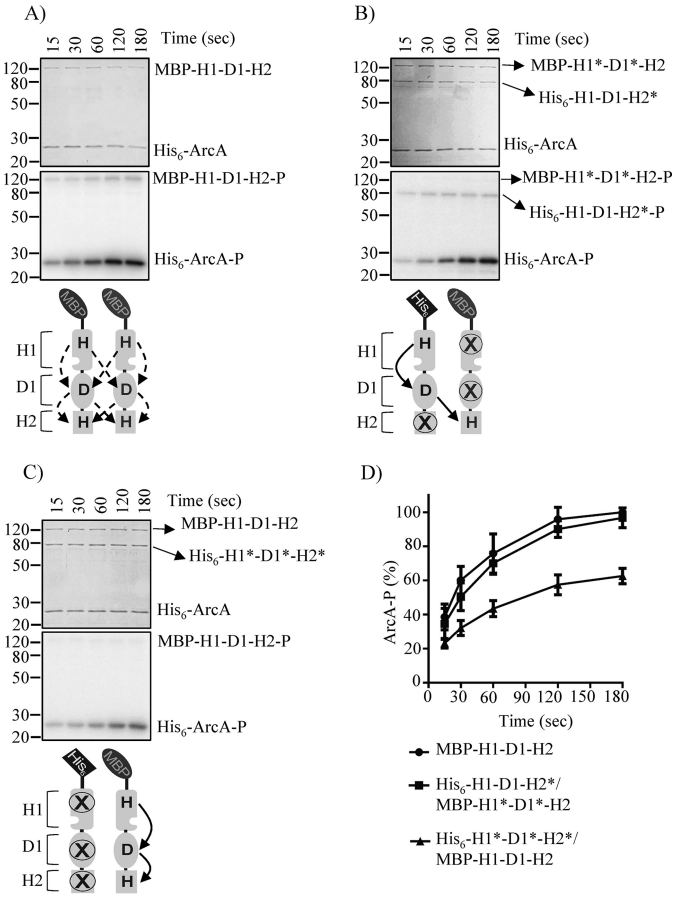

Figure 4. Probing the mode of ~P group transfer from D1 to H2 *in vitro*. Purified ArcA was incubated in a 30-μl reaction mixture, in the presence of [γ-^{32}P]ATP, with purified MBP-H1-D1-H2 (*A*), co-purified His$_6$-H1-D1-H2*/MBP-H1*-D1*-H2 (*B*), or co-purified His$_6$-H1*-D1*-H2*/MBP-H1-D1-H2 (*C*). At the indicated time intervals, 5-μl samples were withdrawn and subjected to SDS-PAGE analysis. Coomassie Blue–stained gels revealing protein bands (*top panels*), the corresponding autoradiograms (*middle panels*), and schemes showing the permitted ~P transfers into ArcB dimers (*bottom panels*) are presented. The molecular mass standard values (kDa) are shown on the *left*, and the position of each polypeptide in the gel is indicated on the *right* of each *panel*. *D*, relative amount of ArcA-P formed, as quantified by densitometric analysis of the autoradiograms. Data represent the averages from at least three independent experiments, and the S.D. values (*error bars*) are indicated.

ArcB^{H292Q,D576A}/ArcB^{wt} heterodimer, a possible explanation could be that the increasing amount of ArcB^{H292Q,D576A} homodimers may lead to ~P transfer from ArcA-P to H2, as has been shown earlier (19), thereby lowering its regulatory activity. Nevertheless, the strain carrying the ArcB^{D576A,H717Q}-expressing plasmid exhibited a more notorious effect. A 40% reduction of reporter expression as compared with that of the ArcB^{H292Q,D576A}-carrying strain was observed under all tested conditions (Fig. 5). It thus appears that, in agreement with the *in vitro* results, the ~P transfer from D1 to H2 has a clear preference for the intermolecular reaction *in vivo*.

Probing the mode of the H2 to D1 ~P transfer for ArcA-P dephosphorylation

The amplitude and duration of an adaptive response depend on the balance between the rates of phosphorylation and dephosphorylation of the response regulator. The sensor kinase ArcB is a bifunctional enzyme that phosphorylates ArcA under stimulatory conditions, and it also dephosphorylates ArcA-P under nonstimulatory conditions (12, 13, 18, 19). The fact that the conserved His^{717} and Asp^{576} are required for both opposing activities of ArcB (18, 19) raises the intriguing possibility that the forward and the reverse phosphorelay do not have the same pattern with respect to inter- and intramolecular phosphoryl group transfers.

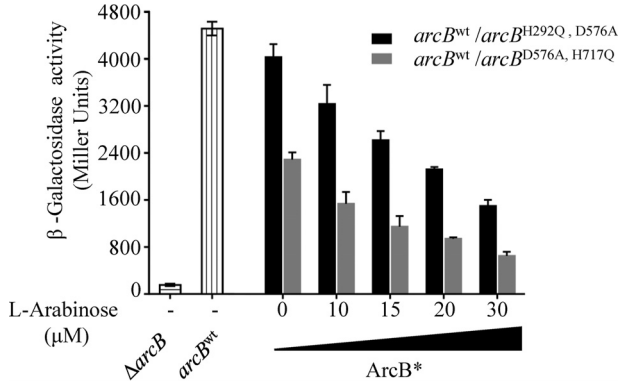

Figure 5. Effect of increasing concentrations of ArcBH^{292Q,D576A} or ArcB^{H576A,H717Q} in an *arcB*^{wt} WT strain on the anaerobic ArcA phosphorylation *in vivo*. Strain ECL5003 (*arcB*^{wt}), carrying plasmid pBAD ArcB^{H292Q,D576A} (*black bars*) or pBADArcB^{D576D,H717A} (*gray bars*) was grown aerobically in LB buffered with 0.1 M MOPS (pH 7.4) and supplemented with 20 mM D-xylose to an A_{600} of 0.1. The culture was split to five screw-cap tubes (filled to the rim) for anaerobic growth, and L-arabinose was added at the indicated concentrations. At the mid-exponential phase of growth (A_{600} of 0.5) β-gal activity was assayed. For comparison purposes, β-gal activities of ECL5003 (*bars* with *vertical lines*) and ECL5004 (*arcB*$^-$) (*bars* with *horizontal lines*) anaerobic cultures are indicated. The data are averages from three independent experiments, and the S.D. values (*error bars*) are indicated.

To test this, His$_6$-ArcA$^{1-136}$ (hereafter referred to as ArcA′), containing the receiver domain but lacking the DNA-binding domain, was purified. ArcA′ was used instead of the full-length His$_6$-ArcA due to the tendency of His$_6$–ArcA-P to aggregate during its purification process (18). The purified protein was incubated with MBP-H1-D1-H2 in the presence of [γ-^{32}P]ATP to generate ArcA′-P. The product, ArcA′-P, was separated from MBP-H1-D1-H2 and [γ-^{32}P]ATP and was used as substrate in phosphatase assays. As observed previously, ArcA′-P was stable, and it maintained in its phosphorylated state during the experiment (Fig. 6*A*) (18). By contrast, both MBP-H1-D1-H2 and MBP-H1*-D1-H2 were shown to rapidly dephosphorylate ArcA-P (Fig. 6*B* and Fig. S3*A*), whereas the His$_6$-H1*-D1-H2* and His$_6$-H1*-D1*-H2* were without effect (Fig. S3, *B* and *C*), in agreement with previous reports (18). On the other hand, MBP-H1*-D1*-H2 was able to receive the ~P from ArcA′-P, but it was unable to release it and, as a consequence, failed to properly dephosphorylate ArcA-P (Fig. S3*D*), as observed previously (18). In contrast, the His$_6$-H1*-D1*-H2*/MBP-H1*-D1-H2 heterodimer, which only permits the intramolecular H2 to D1 ~P transfer, dephosphorylated ArcA′-P at levels similar to those exerted by the WT ArcB, whereas the His$_6$-H1*-D1-H2*/MBP-H1*-D1*-H2 heterodimer, which allows only intermolecular ~P transfer from H2 to D1, dephosphorylated ArcA′-P with a significantly lower rate (Fig. 6, *C–E*). It thus appears that the reverse H2 to D1 ~P transfer occurs preferably intramolecularly.

The mode of ~P transfer from H2 to D1 was then probed *in vivo*, by examining the time lag of ArcA-P dephos-

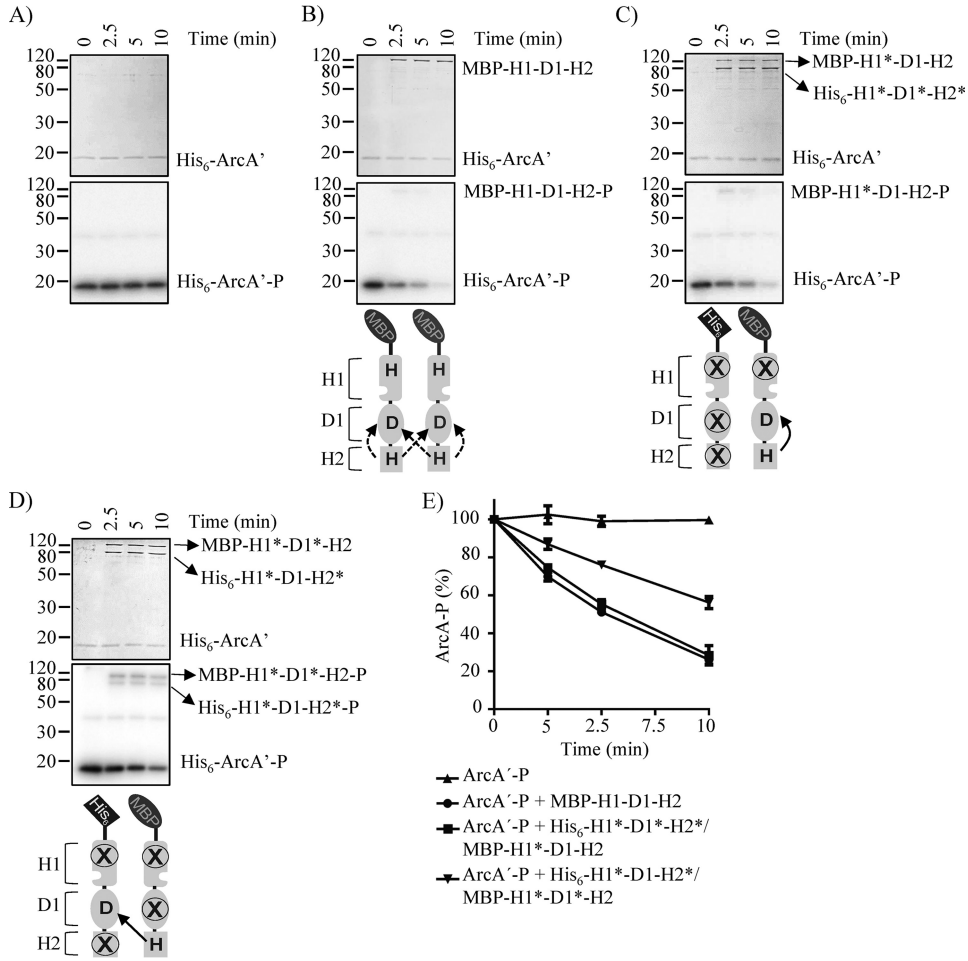

Figure 6. Testing the ArcA′-P dephosphorylation by MBP-H1-D1-H2 and His_6-$ArcB^{78-778}$*/MBP-$ArcB^{78-778}$* dimers. Purified ArcA′-P was incubated alone (*A*) or with MBP-H1-D1-H2 (*B*), His_6-H1*-D1*-H2*/MBP-H1*-D1-H2 (*C*), or His_6-H1*-D1-H2*/MBP-H1*-D1*-H2 (*D*) in 25-μl reaction mixtures. At the indicated time points, 5-μl samples were withdrawn for SDS-PAGE analysis. Coomassie Blue–stained gels revealing protein bands (*top panels*), the corresponding autoradiograms (*middle panels*), and schemes showing the permitted ~P transfers into ArcB dimers (*bottom panels*) are presented. The molecular mass standard values (kDa) are shown on the *left*, and the position of each polypeptide in the gel is indicated on the *right* of each *panel*. *E*, relative amount of ArcA-P formed, as quantified by densitometric analysis of the autoradiograms. Data represent the averages from at least three independent experiments, and the S.D. values (*error bars*) are indicated.

phorylation after a shift from anaerobic to aerobic growth-conditions. To this end, strain ECL5032 ($arcB^{H171Q}$) harboring the $ArcB^{H292Q,D576A}$-expressing plasmid (pEXT22Cm $ArcB^{H292Q,D576A}$) and the isogenic WT strain ECL5002, both carrying the ArcA-P–repressible λΦ(*lldP′-lacZ*) reporter (12, 40), were grown anaerobically in lysogeny broth (LB) supplemented with 20 mM L-lactate to induce expression of the reporter (43). At an A_{600} of ~0.2, a sample was withdrawn, and the expression of the reporter was determined (depicted as 0 min in Fig. 7). As expected, in both strains, the expression of the reporter was very low (Fig. 7), indicative of ArcA-P– dependent reporter repression. This result demonstrates that co-expression of the $arcB^{H717Q}$ and $arcB^{H292Q,D576A}$ mutant alleles fully restores ArcB kinase activity and thus proper $ArcB^{H717Q}$/$ArcB^{H292Q,D576A}$ heterodimer formation. Subsequently, the cultures were shifted to aerobiosis, and the time course of the β-gal activity was followed. An almost immediate increase of reporter expression (Fig. 7) was observed for the strain carrying the WT *arcB* allele, indicating ArcA-P dephosphorylation and release of reporter repression. On the other hand, a retarded and scarce increase of reporter expression was noticed for the

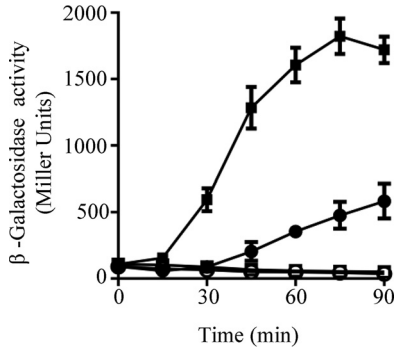

Figure 7. Testing the time lag for ArcA-P dephosphorylation (signal decay) after a shift to nonstimulating conditions. Strain ECL5002 (*squares*) and its isogenic ECL5032 ($arcB^{H171Q}$) strain harboring a plasmid-born $arcB^{H292Q,D576A}$ allele (*circles*), both carrying the λΦ(*lldP′-lacZ*) reporter, were grown anaerobically in LB buffered with 0.1 M MOPS (pH 7.4) and supplemented with 20 mM D-xylose and 20 mM L-lactate. At an A_{600} of 0.2, one aliquot was withdrawn, to measure the β-gal activity (depicted as 0 min), and the rest of the cultures were divided into two: one of the subcultures was kept under anaerobiosis (*open symbols*), serving as control, whereas the other one was shifted to aerobiosis (*filled symbols*), and the time course of the β-gal activity was followed. Data represent the averages from three independent experiments, and the S.D. values (*error bars*) are indicated.

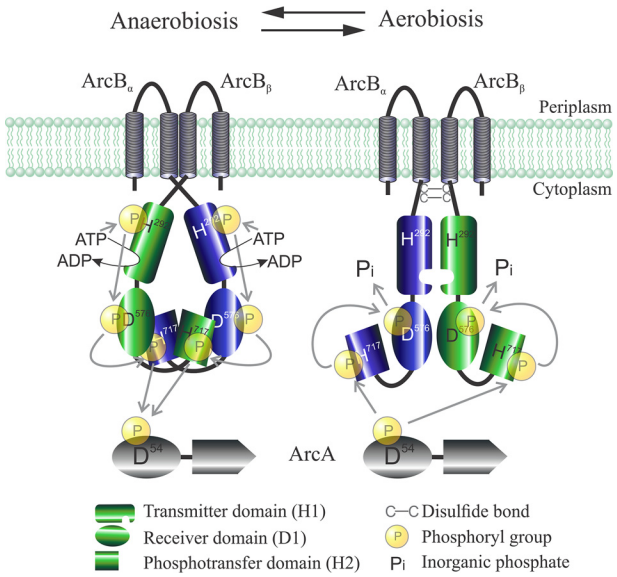

Figure 8. *Graphic representation* of the ArcB/A two-component system showing the proposed modes of ~P group transfer during signal propagation (anaerobiosis) and signal decay (aerobiosis). Under anoxic growth conditions, the ATP-dependent intramolecular autophosphorylation in H1 is followed by a phosphorelay that involves an intramolecular H1 to D1 phosphotransfer and an intermolecular D1 to H2 phosphotransfer. Under oxic growth conditions, disulfide bond–dependent conformational adjustments of the ArcB modules enforce an intramolecular phosphotransfer from H2 to D1 followed by release of ~P as P_i, resulting in ArcA-P dephosphorylation and signal decay.

strain carrying the *arcB*^{H717Q} and *arcB*^{H292Q,D576A} mutant alleles (Fig. 7). Taken together, these results strongly suggest that the reverse ~P transfer during signal decay (*i.e.* from H2 to D1) operates intramolecularly.

Thus, it seems reasonable to conclude that conformational changes of ArcB may affect the mode of ~P transfer between the D1 and H2 domains, thereby discriminating between the two opposing activities (*i.e.* between signal transmission and signal decay).

Discussion

In this study, results from *in vitro* and *in vivo* experiments demonstrate that the His^{292} to Asp^{576} ~P transfer within the ArcB dimer occurs exclusively intramolecularly, whereas the ~P transfer from Asp^{576} to His^{717} occurs preferentially intermolecularly. Finally, the reverse ~P transfer responsible for signal decay, namely from His^{717} to Asp^{576}, appears to have a clear preference for the intramolecular reaction. It is therefore tempting to propose a model in which, during signal propagation, the physiological mode of ~P transfers between the individual ArcB modules occurs intramolecularly from H1 to D1 and intermolecularly from D1 to H2, whereas the reverse ~P transfer during signal decay (*i.e.* from H2 to D1) occurs intramolecularly (Fig. 8).

This model differs from that of a previous study, based on *in vivo* experiments analyzed with mathematical and statistical models, where it was suggested that the mechanism operating in ArcB ~P transfers is dictated by a cooperative or bimolecular mechanism in which all phosphorylation sites of both monomers appear to be required for proper functioning of the ArcB phosphorelay (39). It is worth noting that in these *in vivo* experiments, the ArcB variants were expressed from medium to high copy number plasmids under the control of IPTG-inducible promoters and with the addition of 0.1 mM IPTG. Surprisingly, all combinations, including those in which a WT ArcB was co-expressed with mutant ArcB variants, failed to fully restore a functional phosphorelay. Therefore, it was suggested that all domains and phosphorylation sites in both monomers have to be present if a functional phosphorelay is to be allowed. However, in our hands, co-expression of a chromosomal *arcB*^{H717Q} mutant and a low-copy number plasmid-borne *arcB*^{H292Q,D576A} mutant fully restored the kinase activity of ArcB (Fig. 3*D*), indicating that the mutant proteins do complement not only the WT ArcB activity but also its regulation. Therefore, we could only speculate that, in the earlier study, a possible overproduction of the ArcB mutant variants might have been the cause of the lower ArcA activation. Indeed, it has been demonstrated previously that significant overexpression of proteins can be achieved with plasmid pCA24N, which was used in the above study, with as little as 50 μM IPTG (44). In fact, we have observed that overexpression of a mutant version of ArcB in a WT strain results in a drastic reduction of ArcA-P formation and, thereby, reporter expression (Fig. 5). This, most probably, could be caused by the alteration of the sensor/response regulator concentration balance, in accordance with previous observations for other two-component signal transduction systems (42, 45). Moreover, an intermolecular ~P transfer from H1 to D1 of ArcB, in contrast to our result, was reported in an earlier study. In that study, the mode of ~P transfers involved in the phosphorelay of ArcB was analyzed by complementation of single-phosphorelay mutant proteins in *in vitro* phosphorylation assays, followed by separation of phosphorylated proteins by Phos-Tag SDS-PAGE and detection by Coomassie Blue staining (38). However, the high protein concentrations needed for detection of phosphorylated forms of proteins by Coomassie Blue after Phos-Tag SDS-PAGE separation could increase the incidence of nonspecific phosphorylation and, therefore, weaken the resulting conclusions. In contrast, our *in vitro* assays, using ArcB mutant heterodimers, in addition to the *in vivo* complementation experiments, clearly discard intermolecular H1 to D1 phosphotransfer and demonstrate that only the intramolecular transfer is allowed.

At any rate, the model proposed herein for ArcB (Fig. 8) appears appealing if we consider that the spatio-steric constraints of a given assembly of an ArcB$_\alpha$/ArcB$_\beta$ homodimer should allow only Asp$^{576}{}_\alpha$ or Asp$^{576}{}_\beta$ to be in the vicinity of His$^{292}{}_\alpha$, permitting either an inter- or intramolecular ~P transfer. Likewise, only one His^{717}, the one of either ArcB$_\alpha$ or ArcB$_\beta$, could be in the vicinity of Asp$^{576}{}_\alpha$, permitting only one mode of ~P transfer. Thus, under anoxic growth conditions, the assembly of the ArcB$_\alpha$/ArcB$_\beta$ dimer would permit the intramolecular ~P transfer from H1 to D1 (His$^{292}{}_\alpha \rightarrow$ Asp$^{576}{}_\alpha$ and His$^{292}{}_\beta \rightarrow$ Asp$^{576}{}_\beta$) and the intermolecular ~P transfer from D1 to H2 (Asp$^{576}{}_\alpha \rightarrow$ His$^{717}{}_\beta$ and Asp$^{576}{}_\beta \rightarrow$ His$^{717}{}_\alpha$), favoring the kinase activity of ArcB. On the other hand, under oxic growth conditions, redox-dependent conformational adjustments of the individual modules within the ArcB dimer would permit the intramolecular ~P transfer from H2 to D1 (His$^{717}{}_\alpha \rightarrow$ Asp$^{576}{}_\alpha$ and His$^{717}{}_\beta \rightarrow$ Asp$^{576}{}_\beta$), favoring the phosphatase activity of

ArcB. Such a model provides some insights within the biochemical mechanism that dictates the direction of ~P transfer, thereby differentiating the kinase and phosphatase activities of ArcB. A similar *modus operandi* may also apply to other two-component systems comprising a tripartite sensor kinase. Nevertheless, the attainment and analysis of the ArcB crystallographic structure should be needed to elucidate the conformational adjustments that occur upon changes in the redox conditions and to completely understand the bases of the ArcB ~P transfer pattern.

Experimental procedures

Bacterial strains, plasmids, and growth conditions

The strains and plasmids used in this work are listed in Table S1. Strains IFC2001 and IFC2002 were constructed by P1*vir* transduction of the *fnr*::Tn*10* allele from strain ECL556 (46) into strains ECL5023 and ECL5024 (12), respectively. Plasmids pQE30ArcB$^{78-778}$, pQE30ArcB$^{78-778,H292Q}$ (pMX028), pQE30 ArcB$^{78-778,D576A,H717Q}$, pQE30ArcB$^{78-661,D576A}$, pQE30 ArcB$^{521-778,H717Q}$, pQE30ArcA, and pQE30ArcA$^{1-136}$, used for cloning and/or for expression of His$_6$-ArcB and His$_6$-ArcA derivatives, have been described previously (10, 13, 16, 18, 35). Plasmid pQE30ArcB$^{78-778,D576A}$ was constructed by replacing the BamHI-EcoRV fragment of plasmid pQE30 ArcB$^{78-778}$ with the corresponding restriction fragment of pQE30ArcB$^{78-661,D576A}$. Plasmids pQE30ArcB$^{78-778,H717Q}$ and pQE30ArcB$^{78-778,H292Q,H717Q}$ were constructed by replacing the EcoRV-HindIII fragment of pQE30ArcB$^{78-778}$ and pQE30ArcB$^{78-778,H292Q}$, respectively, with the corresponding fragment of pQE30ArcB$^{521-778,H717Q}$. Plasmid pQE30 ArcB$^{78-778,H292Q,D576A}$ was constructed by replacing the MluI-EcoRV fragment of plasmid pQE30ArcB$^{78-778,H292Q}$ with the corresponding MluI-EcoRV fragment of pQE30ArcB$^{78-778,D576A}$. Plasmid pQE30ArcB$^{78-778,H292Q,D576A,H717Q}$ was created by replacing the MluI-HindIII fragment of plasmid pQE30 ArcB$^{78-778,H292Q}$ with the corresponding fragment of plasmid pQE30ArcB$^{78-778,D576A,H717Q}$. Plasmids pBADHis-ArcB$^{78-778*}$ (where the asterisk refers to specific amino acid replacements; see Table S1), used for L-arabinose–induced expression of His$_6$-ArcB$^{78-778*}$, were constructed by cloning the NdeI-HindIII fragment from the respective pQE30ArcB$^{78-778*}$ between the same restriction sites of plasmid pMX517 (8). Plasmid pMAL-ArcB$^{78-778}$, used for expression of ArcB$^{78-778}$ fused to the maltose-binding protein (MBP-H1-D1-H2), was created by cloning the BamHI-HindIII fragment from pQE30ArcB$^{78-778}$ between the same restriction sites of pMAL-c2x (New England Biolabs). Then the HpaI-HindIII restriction fragment from plasmid pMAL-ArcB$^{78-778}$, containing the MBP-ArcB$^{78-778}$-expressing gene and the *tac* promoter, was cloned between the SmaI and HindIII sites of plasmid pACT3 (41), resulting in pACT3MBP-ArcB$^{78-778}$. Afterward, pACT3MBP-ArcB$^{78-778*}$ plasmids were constructed by replacing the BamHI-HindIII fragment of pACT3MBP-ArcB$^{78-778}$ with the BamHI-HindIII fragment from the corresponding pQE30ArcB$^{78-778*}$ (where the asterisk refers to specific amino acid replacements; see Table S1). High-copy number plasmids carrying full-length *arcB* variants pMX546 (*arcB*^{H292Q}), pMX547 (*arcB*^{H292Q,D576A}), and pMX548 (*arcB*^{D576A,H717Q}) were created by cloning the NruI-HindIII fragment from the corresponding pQE30ArcB$^{78-778*}$ between the NruI and HindIII sites of pMX712 (*arcB*^{wt}) (8). The low-copy number plasmid pEXT22Cm, used for *in vivo* complementation assays, was obtained by cloning the blunt-ended XmnI-ScaI fragment from pACT3 (41), containing the chloramphenicol resistance cassette, into the SspI-restricted pEXT22 (41). Then the BamHI-HindIII fragments from pMX712, pMX546, and pMX547 were cloned between the BamHI and HindIII sites of pEXT22Cm to generate pEXT22CmArcB^{wt}, pEXT22CmArcB^{H292Q}, and pEXT22 CmArcB^{H292Q,D576A}, respectively. Plasmids pBADArcB^{H292Q,D576A} and pBADArcB^{D576D,H717A}, used to express full-length ArcB under the control of the L-arabinose–inducible promoter, were constructed by cloning the NdeI-HindIII restriction fragment from pMX547 and pMX548, respectively, between the NdeI and HindIII sites of pMX517 (8).

Bacteria were routinely cultured at 37 °C in LB. When necessary, media were supplemented with antibiotics, at the following concentrations: chloramphenicol, 20 μg/ml; kanamycin, 50 μg/ml; ampicillin, 100 μg/ml; and tetracycline, 10 μg/ml. For β-galactosidase activity assays, the $\lambda\Phi$(*cydA′-lacZ*)-bearing strains were grown in LB containing 0.1 M MOPS (pH 7.4) and 20 mM D-xylose, whereas the $\lambda\Phi$(*lldP′-lacZ*)-bearing strains were grown in the above medium supplemented with 20 mM L-lactate as inducer.

Purification of His$_6$- and MBP-tagged proteins and phosphorylation assays

Native His$_6$-tagged ArcB$^{78-778}$ variants and His$_6$-ArcA, used in phosphorylation assays, were prepared as described previously (13, 47). MBP-tagged ArcB$^{78-778}$ variants were purified by using amylose resin (New England Biolabs) as affinity matrix according to the instructions provided by the manufacturer. For the co-purification of the His$_6$-/MBP-tagged ArcB versions, strain ECL5012 (*arcB*$^-$) (40) carrying both pBADHis-ArcB$^{78-778*}$ and pACT3MBP-ArcB$^{78-778*}$ (where the asterisk refers to specific amino acid replacements) was grown in 1 liter of LB, supplemented with chloramphenicol and ampicillin, in a rotary shaker at 37 °C until an A_{600} of 0.6. Then the expression of the His$_6$- and MBP-tagged ArcB$^{78-778*}$ was induced by the addition of 1 mM L-arabinose and 0.1 mM IPTG, respectively. Cells were harvested 5 h after induction, and the cell pellet was resuspended in 10 ml of lysis buffer (50 mM sodium phosphate, pH 8.0, 300 mM NaCl, 10 mM imidazole). Finally, the proteins were purified under native conditions by Ni-NTA–agarose affinity chromatography, as described previously (13, 47). Phosphorylation assays were carried out at room temperature in the presence of 40 μM [γ-^{32}P]ATP (specific activity, 2 Ci mmol^{-1}; New England Nuclear), 33 mM HEPES (pH 7.5), 50 mM KCl, 5 mM $MgCl_2$, 1 mM DTT, 0.1 mM EDTA, and 10% glycerol. 5 pmol of purified ArcB$^{78-778*}$ (His$_6$- or MBP-tagged) or 10 pmol of co-purified His$_6$- and MBP-tagged ArcB$^{78-778*}$ and 50 pmol of His$_6$-ArcA were used in each phosphorylation assay. The phosphorylation reactions were initiated by the addition of [γ-^{32}P]ATP, and samples were withdrawn and mixed with SDS sample buffer after 15, 30, 60, 120, and 180 s and subject to

analysis by SDS-PAGE on 12% polyacrylamide gels. The radioactivity of proteins resolved in the gels was analyzed by exposing to a Storage Phosphor Screen and scanning by a Typhoon FLA7000 biomolecular imager (GE Healthcare). The intensity of individual band signals was estimated using the ImageQuant version 5.2 software (Molecular Dynamics).

Isolation of His-ArcA$^{1-136}$-P and dephosphorylation assays

Phosphorylation of ArcA$^{1-136}$ and dephosphorylation assays were carried out as described previously (10, 47). Briefly, a 20-μl reaction mixture containing phosphorylation buffer (33 mM HEPES at pH 7.5, 50 mM KCl, 5 mM $MgCl_2$, 1 mM DTT, 0.1 mM EDTA, and 10% glycerol), ArcA$^{1-136}$ (20 mM, purified as a His_6-tagged peptide as above), MBP-ArcB$^{78-778}$ (2 mM), and 40 μM [γ-^{32}P]ATP (specific activity 2 Ci/mmol) was incubated at room temperature. After 10 min, the reaction was stopped by the addition of 100 μl of buffer A, containing 50 mM Tris-HCl at pH 7.0, 150 mM KCl, 5 mM EDTA, and 3% Triton X-100. Separation of ArcA$^{1-136}$-P from MBP-ArcB$^{78-778}$-P was achieved by ultrafiltration using a Nanosep 30 K device (Pallfiltron), which retains MBP-ArcB$^{78-778}$ but not ArcA$^{1-136}$-P, ATP, and P_i. The eluate was then passed through a Nanosep 10K device (Pallfiltron), washed four times with 500 ml of buffer A to remove ATP and Pi, and once with 500 ml of dephosphorylation buffer (33 mM HEPES at pH 7.5, 50 mM KCl, 5 mM $MgCl_2$, 0.1 mM EDTA, and 10% glycerol). The retained material containing ArcA$^{1-136}$-^{32}P (essentially free of MBP-ArcB$^{78-778}$, ATP, and P_i) was recovered in 200 ml of dephosphorylation buffer, aliquoted, and used in dephosphorylating assays. Dephosphorylation reactions were carried out at room temperature in mixtures of 25 μl containing 50 pmol of His_6-ArcA$^{1-136}$-^{32}P and 5 pmol of MBP-ArcB$^{78-778}$ or 10 pmol of co-purified ArcB heterodimers in dephosphorylation buffer. At various time points, a 5-μl sample was withdrawn, mixed with 5 μl of SDS sample buffer, and analyzed by SDS-PAGE on 15% polyacrylamide gels. The radioactivity of proteins resolved in the gels was analyzed by using a PhosphorImager (Molecular Dynamics).

β-Galactosidase activity assay

In general, for aerobic growth, cells were cultured in 10–50 ml of medium in 250-ml baffled flasks at 37 °C with shaking (300 rpm), whereas for anaerobic growth, cells were cultured in a screw-capped tube filled with medium up to the rim at 37 °C and stirred by a magnet. For the aerobiosis to anaerobiosis shift, cells were aerobically grown and, at an A_{600} of 0.2, part of the culture was transferred to five prewarmed screw-capped tubes, filled up to the rim, and stirred by a magnet. The rest of the aerobic culture was further incubated with shaking at the same temperature. The time course of the experiment was followed by taking a sample from a filled screw-capped tube (anaerobiosis) and from the baffled flasks (aerobiosis) at each chosen time. For the anaerobiosis-to-aerobiosis shift, cells were cultured in seven screw-capped tubes filled with medium up to the rim at 37 °C and stirred by a magnet. At an A_{600} of 0.2, the content of a tube was passed to a 250-ml prewarmed baffled flask and incubated with shaking at the same temperature. Samples from aerobic and anaerobic cultures (the rest of the screw-capped tubes) were withdrawn at each chosen time after the shift. β-gal activity was assayed and expressed in Miller units as described previously (48).

Western blotting

Cells were harvested from cultures by centrifugation during mid-exponential growth. The cell pellet was resuspended in sample buffer and separated by SDS-PAGE (10% polyacrylamide gel), and the proteins were transferred to a Hybond-ECL filter (Amersham Biosciences). The filter was equilibrated in TTBS buffer (25 mM Tris, 150 mM NaCl, and 0.05% Tween 20) for 10 min and incubated in blocking buffer (1% milk in TTBS) for 1 h at room temperature. ArcB polyclonal antibodies, raised against His_6-ArcB$^{78-520}$ (12), were added at a dilution of 1:10,000 and incubated for 1 h at room temperature. The bound antibody was detected by using anti-rabbit IgG antibody conjugated to horseradish peroxidase and the ECL detection system (Amersham Biosciences).

Author contributions—J. L. T.-M., A. F. A., and D. G. conceptualization; J. L. T.-M., G. R. P.-S., H. S.-J., and C. R. investigation; J. L. T.-M., G. R. P.-S., H. S.-J., and C. R. methodology; A. F. A. and D. G. supervision; A. F. A. and D. G. funding acquisition; A. F. A. writing-original draft; D. G. writing-review and editing.

Acknowledgments—We thank Diego González-Halphen and Bertha Michel for critically reading the manuscript.

References

1. Georgellis, D., Kwon, O., Lin, E. C., Wong, S. M., and Akerley, B. J. (2001) Redox signal transduction by the ArcB sensor kinase of *Haemophilus influenzae* lacking the PAS domain. *J. Bacteriol.* **183,** 7206–7212 CrossRef Medline
2. Jung, W. S., Jung, Y. R., Oh, D. B., Kang, H. A., Lee, S. Y., Chavez-Canales, M., Georgellis, D., and Kwon, O. (2008) Characterization of the Arc two-component signal transduction system of the capnophilic rumen bacterium *Mannheimia succiniciproducens*. *FEMS Microbiol. Lett.* **284,** 109–119 CrossRef Medline
3. Malpica, R., Sandoval, G. R., Rodríguez, C., Franco, B., and Georgellis, D. (2006) Signaling by the Arc two-component system provides a link between the redox state of the quinone pool and gene expression. *Antioxid. Redox Signal.* **8,** 781–795 CrossRef Medline
4. Lynch, A. S., and Lin, E. C. (1996) Regulation of gene expression in *Escherichia coli*. in *Escherichia coli and Salmonella: Cellular and Molecular Biology* (Neidhardt, F. C., Curtis, R., Ingraham, A. L., Lin, E. C. C., Low, K. B., Magasanik, B., Reznikoff, W. S., Riley, M., Schaechter, M., and Umbarger, H. E., eds) pp. 1526–1538, American Society for Microbiology, Washington, D. C.
5. Iuchi, S., and Lin, E. C. (1988) *arcA* (*dye*), a global regulatory gene in *Escherichia coli* mediating repression of enzymes in aerobic pathways. *Proc. Natl. Acad. Sci. U.S.A.* **85,** 1888–1892 CrossRef Medline
6. Iuchi, S., Matsuda, Z., Fujiwara, T., and Lin, E. C. (1990) The *arcB* gene of *Escherichia coli* encodes a sensor-regulator protein for anaerobic repression of the *arc* modulon. *Mol. Microbiol.* **4,** 715–727 CrossRef Medline
7. Ishige, K., Nagasawa, S., Tokishita, S., and Mizuno, T. (1994) A novel device of bacterial signal transducers. *EMBO J.* **13,** 5195–5202 Medline
8. Nuñez Oreza, L. A., Alvarez, A. F., Arias-Olguín, I. I., Torres Larios, A., and Georgellis, D. (2012) The ArcB leucine zipper domain is required for proper ArcB signaling. *PLoS One* **7,** e38187 CrossRef Medline
9. Zhulin, I. B., Taylor, B. L., and Dixon, R. (1997) PAS domain S-boxes in Archaea, Bacteria and sensors for oxygen and redox. *Trends Biochem. Sci.* **22,** 331–333 CrossRef Medline
10. Georgellis, D., Kwon, O., and Lin, E. C. (1999) Amplification of signaling activity of the Arc two-component system of *Escherichia coli* by anaerobic

metabolites: an *in vitro* study with different protein modules. *J. Biol. Chem.* **274,** 35950–35954 CrossRef Medline
11. Rodriguez, C., Kwon, O., and Georgellis, D. (2004) Effect of D-lactate on the physiological activity of the ArcB sensor kinase in *Escherichia coli*. *J. Bacteriol.* **186,** 2085–2090 CrossRef Medline
12. Kwon, O., Georgellis, D., and Lin, E. C. (2000) Phosphorelay as the sole physiological route of signal transmission by the Arc two-component system of *Escherichia coli*. *J. Bacteriol.* **182,** 3858–3862 CrossRef Medline
13. Georgellis, D., Lynch, A. S., and Lin, E. C. (1997) *In vitro* phosphorylation study of the Arc two-component signal transduction system of *Escherichia coli*. *J. Bacteriol.* **179,** 5429–5435 CrossRef Medline
14. Gunsalus, R. P., and Park, S. J. (1994) Aerobic-anaerobic gene regulation in *Escherichia coli*: control by the ArcAB and Fnr regulons. *Res. Microbiol.* **145,** 437–450 CrossRef Medline
15. Liu, X., and De Wulf, P. (2004) Probing the ArcA-P modulon of *Escherichia coli* by whole genome transcriptional analysis and sequence recognition profiling. *J. Biol. Chem.* **279,** 12588–12597 CrossRef Medline
16. Lynch, A. S., and Lin, E. C. (1996) Transcriptional control mediated by the ArcA two-component response regulator protein of *Escherichia coli*: characterization of DNA binding at target promoters. *J. Bacteriol.* **178,** 6238–6249 CrossRef Medline
17. Alvarez, A. F., Malpica, R., Contreras, M., Escamilla, E., and Georgellis, D. (2010) Cytochrome *d* but not cytochrome *o* rescues the toluidine blue growth sensitivity of *arc* mutants of *Escherichia coli*. *J. Bacteriol.* **192,** 391–399 CrossRef Medline
18. Georgellis, D., Kwon, O., De Wulf, P., and Lin, E. C. (1998) Signal decay through a reverse phosphorelay in the Arc two-component signal transduction system. *J. Biol. Chem.* **273,** 32864–32869 CrossRef Medline
19. Peña-Sandoval, G. R., Kwon, O., and Georgellis, D. (2005) Requirement of the receiver and phosphotransfer domains of ArcB for efficient dephosphorylation of phosphorylated ArcA *in vivo*. *J. Bacteriol.* **187,** 3267–3272 CrossRef Medline
20. Kwon, O., Georgellis, D., and Lin, E. C. (2003) Rotational on-off switching of a hybrid membrane sensor kinase Tar-ArcB in *Escherichia coli*. *J. Biol. Chem.* **278,** 13192–13195 CrossRef Medline
21. Georgellis, D., Kwon, O., and Lin, E. C. (2001) Quinones as the redox signal for the Arc two-component system of bacteria. *Science* **292,** 2314–2316 CrossRef Medline
22. Alvarez, A. F., Rodriguez, C., and Georgellis, D. (2013) Ubiquinone and menaquinone electron carriers represent the yin and yang in the redox regulation of the ArcB sensor kinase. *J. Bacteriol.* **195,** 3054–3061 CrossRef Medline
23. Malpica, R., Franco, B., Rodriguez, C., Kwon, O., and Georgellis, D. (2004) Identification of a quinone-sensitive redox switch in the ArcB sensor kinase. *Proc. Natl. Acad. Sci. U.S.A.* **101,** 13318–13323 CrossRef Medline
24. Bekker, M., Alexeeva, S., Laan, W., Sawers, G., Teixeira de Mattos, J., and Hellingwerf, K. (2010) The ArcBA two-component system of *Escherichia coli* is regulated by the redox state of both the ubiquinone and the menaquinone pool. *J. Bacteriol.* **192,** 746–754 CrossRef Medline
25. Tomomori, C., Tanaka, T., Dutta, R., Park, H., Saha, S. K., Zhu, Y., Ishima, R., Liu, D., Tong, K. I., Kurokawa, H., Qian, H., Inouye, M., and Ikura, M. (1999) Solution structure of the homodimeric core domain of *Escherichia coli* histidine kinase EnvZ. *Nat. Struct. Biol.* **6,** 729–734 CrossRef Medline
26. Tanaka, T., Saha, S. K., Tomomori, C., Ishima, R., Liu, D., Tong, K. I., Park, H., Dutta, R., Qin, L., Swindells, M. B., Yamazaki, T., Ono, A. M., Kainosho, M., Inouye, M., and Ikura, M. (1998) NMR structure of the histidine kinase domain of the *E. coli* osmosensor EnvZ. *Nature* **396,** 88–92 CrossRef Medline
27. West, A. H., and Stock, A. M. (2001) Histidine kinases and response regulator proteins in two-component signaling systems. *Trends Biochem. Sci.* **26,** 369–376 CrossRef Medline
28. Alvarez, A. F., Barba-Ostria, C., Silva-Jiménez, H., and Georgellis, D. (2016) Organization and mode of action of two component system signaling circuits from the various kingdoms of life. *Environ. Microbiol.* **18,** 3210–3226 CrossRef Medline
29. Stock, A. M., Robinson, V. L., and Goudreau, P. N. (2000) Two-component signal transduction. *Annu. Rev. Biochem.* **69,** 183–215 CrossRef Medline
30. Yang, Y., and Inouye, M. (1991) Intermolecular complementation between two defective mutant signal-transducing receptors of *Escherichia coli*. *Proc. Natl. Acad. Sci. U.S.A.* **88,** 11057–11061 CrossRef Medline
31. Ninfa, E. G., Atkinson, M. R., Kamberov, E. S., and Ninfa, A. J. (1993) Mechanism of autophosphorylation of *Escherichia coli* nitrogen regulator II (NRII or NtrB): trans-phosphorylation between subunits. *J. Bacteriol.* **175,** 7024–7032 CrossRef Medline
32. Casino, P., Rubio, V., and Marina, A. (2009) Structural insight into partner specificity and phosphoryl transfer in two-component signal transduction. *Cell* **139,** 325–336 CrossRef Medline
33. Swanson, R. V., Bourret, R. B., and Simon, M. I. (1993) Intermolecular complementation of the kinase activity of CheA. *Mol. Microbiol.* **8,** 435–441 CrossRef Medline
34. Cotter, P. A., and Jones, A. M. (2003) Phosphorelay control of virulence gene expression in *Bordetella*. *Trends Microbiol.* **11,** 367–373 CrossRef Medline
35. Peña-Sandoval, G. R., and Georgellis, D. (2010) The ArcB sensor kinase of *Escherichia coli* autophosphorylates by an intramolecular reaction. *J. Bacteriol.* **192,** 1735–1739 CrossRef Medline
36. Jourlin, C., Ansaldi, M., and Méjean, V. (1997) Transphosphorylation of the TorR response regulator requires the three phosphorylation sites of the TorS unorthodox sensor in *Escherichia coli*. *J. Mol. Biol.* **267,** 770–777 CrossRef Medline
37. Uhl, M. A., and Miller, J. F. (1996) Integration of multiple domains in a two-component sensor protein: the *Bordetella pertussis* BvgAS phosphorelay. *EMBO J.* **15,** 1028–1036 Medline
38. Kinoshita-Kikuta, E., Kinoshita, E., Eguchi, Y., and Koike, T. (2016) Validation of *cis* and *trans* modes in multistep phosphotransfer signaling of bacterial tripartite sensor kinases by using Phos-Tag SDS-PAGE. *PLoS One* **11,** e0148294 CrossRef Medline
39. Jovanovic, G., Sheng, X., Ale, A., Feliu, E., Harrington, H. A., Kirk, P., Wiuf, C., Buck, M., and Stumpf, M. P. H. (2015) Phosphorelay of non-orthodox two component systems functions through a bi-molecular mechanism *in vivo*: the case of ArcB. *Mol. BioSyst.* **11,** 1348–1359 CrossRef Medline
40. Kwon, O., Georgellis, D., Lynch, A. S., Boyd, D., and Lin, E. C. (2000) The ArcB sensor kinase of *Escherichia coli*: genetic exploration of the transmembrane region. *J. Bacteriol.* **182,** 2960–2966 CrossRef Medline
41. Dykxhoorn, D. M., St Pierre, R., and Linn, T. (1996) A set of compatible tac promoter expression vectors. *Gene* **177,** 133–136 CrossRef Medline
42. Goulian, M. (2010) Two-component signaling circuit structure and properties. *Curr. Opin. Microbiol.* **13,** 184–189 CrossRef Medline
43. Dong, J. M., Taylor, J. S., Latour, D. J., Iuchi, S., and Lin, E. C. (1993) Three overlapping lct genes involved in L-lactate utilization by *Escherichia coli*. *J. Bacteriol.* **175,** 6671–6678 CrossRef Medline
44. Soo, V. W. C., Hanson-Manful, P., and Patrick, W. M. (2011) Artificial gene amplification reveals an abundance of promiscuous resistance determinants in *Escherichia coli*. *Proc. Natl. Acad. Sci. U.S.A.* **108,** 1484–1489 CrossRef Medline
45. Batchelor, E., and Goulian, M. (2003) Robustness and the cycle of phosphorylation and dephosphorylation in a two-component regulatory system. *Proc. Natl. Acad. Sci. U.S.A.* **100,** 691–696 CrossRef Medline
46. Fu, H.-A., Iuchi, S., and Lin, E. C. C. (1991) The requirement of ArcA and Fnr for peak expression of the cyd operon in *Escherichia coli* under microaerobic conditions. *Mol. Gen. Genet.* **226,** 209–213 Medline
47. Alvarez, A. F., and Georgellis, D. (2010) *In vitro* and *in vivo* analysis of the ArcB/A redox signaling pathway. *Methods Enzymol.* **471,** 205–228 CrossRef Medline
48. Miller, J. H. (1972) β-Galactosidase assay. in *Experiments in Molecular Genetics*, pp. 352–355, Cold Spring Harbor Laboratory, Cold Spring Harbor, NY